

Journal of Biomedical Optics

SPIEDigitalLibrary.org/jbo

Imaging tumor hypoxia by near-infrared fluorescence tomography

Nrusingh C. Biswal
Christopher Pavlik
Michael B. Smith
Andres Aguirre
Yan Xu
Saeid Zanganeh
Liisa T. Kuhn
Kevin P. Claffey
Quing Zhu

Imaging tumor hypoxia by near-infrared fluorescence tomography

Nrasingh C. Biswal,^a Christopher Pavlik,^b Michael B. Smith,^b Andres Aguirre,^a Yan Xu,^a Saeid Zanganeh,^a Liisa T. Kuhn,^c Kevin P. Claffey,^d and Quing Zhu^a

^aUniversity of Connecticut, Department of Electrical and Computer Engineering, Storrs, Connecticut 06269

^bUniversity of Connecticut, Department of Chemistry, Storrs, Connecticut 06269

^cUniversity of Connecticut Health Center, Department of Reconstructive Sciences, Farmington, Connecticut 06030

^dUniversity of Connecticut Health Center, Department of Cell Biology, Farmington, Connecticut 06030

Abstract. We have developed a novel nitroimidazole indocyanine dye conjugate for tumor-targeted hypoxia fluorescence tomography. The hypoxia probe has been evaluated *in vitro* using tumor cell lines and *in vivo* with tumor targeting in mice. The *in vitro* cell studies were performed to assess fluorescence labeling differences between hypoxia and normoxia conditions. When treated with the hypoxia probe, a fluorescence emission ratio of 2.5-fold was found between the cells incubated under hypoxia compared to the cells in normoxia condition. Hypoxia specificity was also confirmed by comparing the cells treated with indocyanine dye alone. *In vivo* tumor targeting in mice showed that the fluorescence signals measured at the tumor site were twice those at the normal site after 150 min post-injection of the hypoxia probe. On the other hand, the fluorescence signals measured after injection of indocyanine dye were the same at tumor and normal sites. *In vivo* fluorescence tomography images of mice injected with the hypoxia probe showed that the probe remained for more than 5 to 7 h in the tumors, however, the images of mice injected with indocyanine only dye confirmed that the unbound dye washed out in less than 3 h. These findings are supported with fluorescence images of histological sections of tumor samples using a Li-COR scanner and immunohistochemistry technique for tumor hypoxia. © 2011 Society of Photo-Optical Instrumentation Engineers (SPIE). [DOI: 10.1117/1.3589348]

Keywords: tumor hypoxia; fluorescence imaging; indocyanine green; 2-nitroimidazole.

Paper 10407RR received Jul. 20, 2010; revised manuscript received Apr. 8, 2011; accepted for publication Apr. 19, 2011; published online Jun. 14, 2011.

1 Introduction

Most solid tumors contain a tumor-specific microenvironment that is characterized by low oxygen partial pressure (pO_2) and low pH.^{1–5} Inadequate nutrient and oxygen supply results from the chaotic and distorted tumor vascular network formed during pathological angiogenesis. Tumor hypoxia is a major prognostic indicator of poor prognosis and also participates in resistance to chemotherapeutic drugs. For tumor cells within the hypoxia microenvironment, which occurs as they outgrow their vascular supply, their growth rate slows and conventional chemotherapy that targets cell proliferation are no longer effective. One of the biggest challenges faced by oncologists is to identify the best treatment for each cancer patient that will be personalized to the needs of that particular patient. The extent of tumor hypoxia, which varies from patient to patient, may be a measure of resistance to therapy and intratumoral heterogeneity that are selective to individual patients, especially with metastatic lesions. Developing the ability to image hypoxia in tumors could identify those patients that may be resistant to traditional therapies. Such patients may then be identified for more aggressive or targeted therapies soon after diagnosis, which may have a significant impact on their survival.³

Several researchers have used oxygen electrodes to measure oxygen partial pressure (pO_2) in accessible tumors, most

commonly cervix⁶ and head and neck.⁷ However, the use of electrodes is limited for measuring pO_2 in larger deeply located tumors, such as breast cancers. The best measure of hypoxia would use a molecular probe that is dependent upon the level of O_2 , and exhibits a highly sensitive output. In addition, the probe should be delivered to all cells equally independent of vascular flow. Nitroimidazoles are a commonly studied class of molecular probes that meet these criteria since they diffuse freely in the body and are irreversibly trapped by nucleophilic covalent binding to proteins in environments of low pO_2 ($<1.5\% O_2$).⁸ Among all the imidazole compounds, 2-nitroimidazoles have higher electron affinities and are the most commonly used hypoxia markers labeled with positron emission tomography (PET) radionuclides such as ¹⁸F or ¹²⁴I (Refs. 9 and 10). Labeling with multiple ¹⁹F atoms has also been used for magnetic resonance imaging (MRI) detection of cancers.¹¹ Problems associated with PET radionuclides include low resolution, high background counts, and the use of radioactive tracers. In addition, both PET and MRI systems are expensive for routine clinical use in longitudinal imaging assessments over the course of neoadjuvant chemotherapy; thus, new approaches are needed.

Near-infrared (NIR) fluorescence diffuse optical tomography (FDOT) has tremendous potential for probing tumor molecular markers associated with tumor proliferation, growth, and metastasis.^{12–16} In FDOT, a NIR fluorescent probe is administered, and the irradiation with NIR light allows collection of the

Address all correspondence to: Quing Zhu, University of Connecticut, Department of Electrical and Computer Engineering, Storrs, Connecticut 06269. Tel: 860-486-5523; Fax: 860-486-2447; E-mail: zhu@enr.uconn.edu.

emitted fluorescence signals by detectors or a charge coupled device (CCD) camera for tomographic reconstruction of the 3D imaging volume. This technique is capable of imaging targets at depths up to 2.0 to 3.0 cm from the skin surface when the sources and detectors are employed in reflection geometry. The resolution depends on tissue scattering properties and system signal-to-noise ratio. In general, targets of several millimeters to 1 cm can be resolved. FDOT has been successfully used for imaging molecular probes in small animals and for exogenous contrast agents in human brain and breast lesions.^{12–15} Optical imaging systems offer the advantages of low cost, portability, and can be used repeatedly for longitudinal imaging in outpatient clinical settings. To the best of our knowledge, there are no hypoxia probes for FDOT imaging of tumor hypoxia in the NIR spectrum (700 to 850 nm). Among the NIR fluorescence dyes reported in the literature, indocyanine green (ICG) is the only FDA approved agent that can be used for human subjects due to the very low toxicity and high absorbance in the NIR spectrum. Several breast cancer studies have used ICG absorption or fluorescence to enhance tumor contrast.^{13,14} However, ICG functions as a nonspecific fluorescent dye and it is washed out of the body and tumor sites in less than 10 to 20 min, as would be expected for a small nonreactive dye.

The lack of effective hypoxia imaging probes for use in FDOT in the near-infrared spectrum inspired our synthesis of novel dye-conjugates that link an FDA approved compound, a 2-nitroimidazole derivative, and a *bis*-carboxylic acid derivative

of ICG.^{17,18} The details on dye synthesis procedures, photo-physical and chemical properties, and optical stability of the compounds are explained in Refs. 17 and 18. Briefly, both the *bis*-carboxylic acid ICG derivative and 2-nitroimidazole-ICG have the excitation peak at 755 nm and fluorescent emission peak at 778 nm with a quantum yield of 0.088. In this article, we present the validation of hypoxia targeting and the binding sensitivity of the prototype 2-nitroimidazole-ICG hypoxia marker, with the *bis*-carboxylic acid ICG derivative as a reference (hereafter cited as ICG). We also present *in vivo* hypoxia monitoring and tomography imaging studies using murine tumor models. Fluorescence images of histological sections of tumor samples using a Li-COR scanner and immuno-histochemistry stains for tumor hypoxia using HypoxyprobeTM-1 are presented.

2 Materials and Methods

Hypoxia-dependent targeting of the conjugates were assessed *in vitro* using 4T1 breast cancer cells. Four dishes, each having approximately one million tumor cells, were evaluated first. Two of the four dishes were treated with 5 μ M ICG and the other two were treated with 5 μ M of the 2-nitroimidazole-ICG conjugate. It is noted here that this particular ICG derivative does not form multimers at the concentrations that we used in the *in vitro* and *in vivo* experiments. One dish from each group was incubated in normoxic (5% CO₂, 95% air, 37 °C) conditions and the other two in hypoxic (5% CO₂, 1% O₂, 94% N₂, 37 °C) conditions.

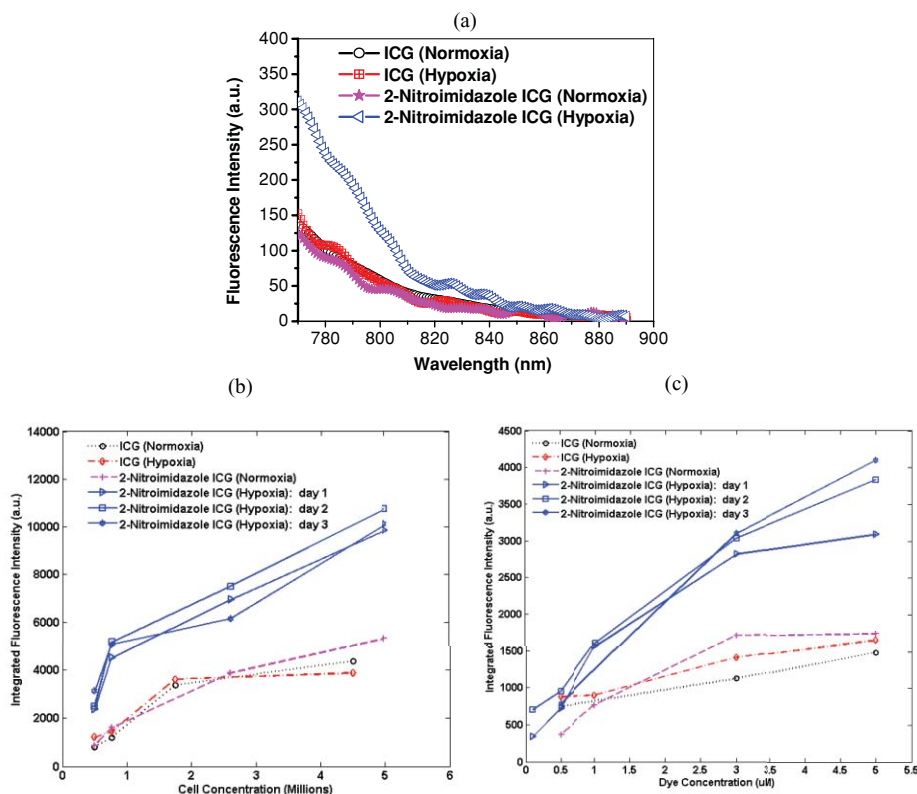


Fig. 1 (a) Fluorescence spectra of ICG and 2-nitroimidazole-ICG treated with normoxia and hypoxia as shown in the corresponding labels, 1 million cells, 5 μ M dye concentration. (b) Integrated fluorescence intensity versus the cell concentration of ICG and 2-nitroimidazole-ICG treated with normoxia and hypoxia as shown in the corresponding labels, 5 μ M dye concentration. (c) Integrated fluorescence intensity versus dye concentration, with normoxia and hypoxia as shown in the corresponding labels, cell density of 1 million. The labels as day 1, day 2, and day 3, for 2-nitroimidazole ICG (Hypoxia) in (b) and (c) are the measurements repeated on three different days.

The gas mixture was customized by Airgas East (Cheshire, Connecticut). After 3 to 4 hours of incubation in the hypoxic chamber,¹⁹ the cell medium oxygenation degraded from 90% to 10%, which were the oxygenation levels commonly observed in normoxic and hypoxic tissue microenvironments. After incubation, dishes were washed twice in phosphate buffer saline (PBS) to remove the unbound molecules and the fluorescence spectra were measured by using a fluorescence spectrophotometer (Varian Analytical Instruments, Walnut Creek, California). Because the fluorescence spectra measured from treated cells were weak, we have used the integrated fluorescence intensity which was calculated as the area under the fluorescence spectra in the wavelength range of 770 to 890 nm for our analysis.

The capacity for the 2-nitroimidazole-ICG to target tumors *in vivo* was tested using a murine tumor model (4T1 mammary cancer cells grown in Balb/c mice). The animal protocol was approved by the Institutional Animal Care and Use Committee of the University of Connecticut. 4T1 breast cancer cells (1×10^5) were injected into the lower right mammary fat-pad of 7-week-old Balb/c female mice. Two sets of experiments were performed when tumors reached approximately 10 mm in the largest dimension, 2 to 3 weeks post-innoculation. In the first set of experiments, tumor uptake and dye wash out time was measured in 4 mice using two pairs of source-detector assemblies placed on top of the tumor and the normal sites. In the second set of experiments, fluorescence tomography imaging experiments were performed in three mice using a hand-held probe with mice tumor submerged in the intralipid solution.¹⁶ All the experiments were performed under anesthesia by the inhalation of 1.5% isoflurane. A commercially available 2-nitroimidazole hypoxia marker, HypoxyprobeTM-1 from HPI Inc., was used to visualize the hypoxia tumor areas using an immuno-histochemistry technique. Based on the protocol provided by the company, 45 min before the animal was euthanized, 1.5 mg of HypoxyprobeTM-1 diluted in 100 μ l of 0.9% saline solution was injected. Immediately after the animal was euthanized, the tumor was harvested, mounted using OCT (optimum cutting temperature) gel, and then frozen under -80 °C. Frozen samples were cut in 10 to 20 μ m thin slices and adjacent slices were processed with: a. antibody kit from Vector Laboratories (California) to visualize the HypoxyprobeTM-1; b. H&E stained to visualize the tumor morphology; and c. high resolution fluorescence imaging performed to visualize the presence of the dye in tumor areas. In the tumor sample fluorescence imaging, sections were dried and imaged using an Odyssey Infrared Imaging System (Li-COR Biosciences, Nebraska). This instrument provides scan resolution ranges of 21 to 339 μ m. The fluorescence images obtained for this work were acquired at 21 μ m which was the highest resolution. The excitation channel selected was 785 nm and emission was 820 nm with bandwidth of 40 to 50 nm. The images were obtained using the analysis software provided by the company.²⁰ To visualize the hypoxic regions, part of the tumor tissue was fixed in 4% paraformaldehyde overnight. Slides were blocked in 5% normal goat serum for 1 h at room temperature. Slides were incubated with a primary antibody, mouse IgG monoclonal antibody (MAb1) diluted in 5% normal goat serum (1:50 Hypoxyprobe, HPI Inc., Massachusetts), washed, and a secondary biotinylated goat-anti-mouse IgG antibody was applied. The avidin-biotin peroxidase complex method was used

and staining was visualized using the DAB chromophore (DAB, ABC; Vector Laboratories, California).^{21,22}

3 Results

As shown in Fig. 1(a), the fluorescence emission was 2.5 times higher for cells treated with 2-nitroimidazole-ICG in hypoxia as compared with that in normoxia; while fluorescence intensity of ICG treated dishes were the same for both hypoxia and normoxia conditions. The results demonstrate that more 2-nitroimidazole-ICG was trapped in/on the tumor cells under the hypoxia conditions. The binding sensitivity increases with cell concentration (at fixed dye concentration of 5 μ M) as expected, because of the expected cell-dependent consumption of the available oxygen [see Figure 1(b)]. The integrated fluorescence intensity increases linearly with cell density for cells treated with 2-nitroimidazole-ICG under hypoxic conditions. Dye concentration effects are shown in Fig. 1(c). At the 1 μ M concentration, the fluorescence intensity of 2-nitroimidazole-ICG is about 2 times higher under hypoxia as compared to that under normoxia. At the 5 μ M concentration, the fluorescence intensity of the 2-nitroimidazole-ICG

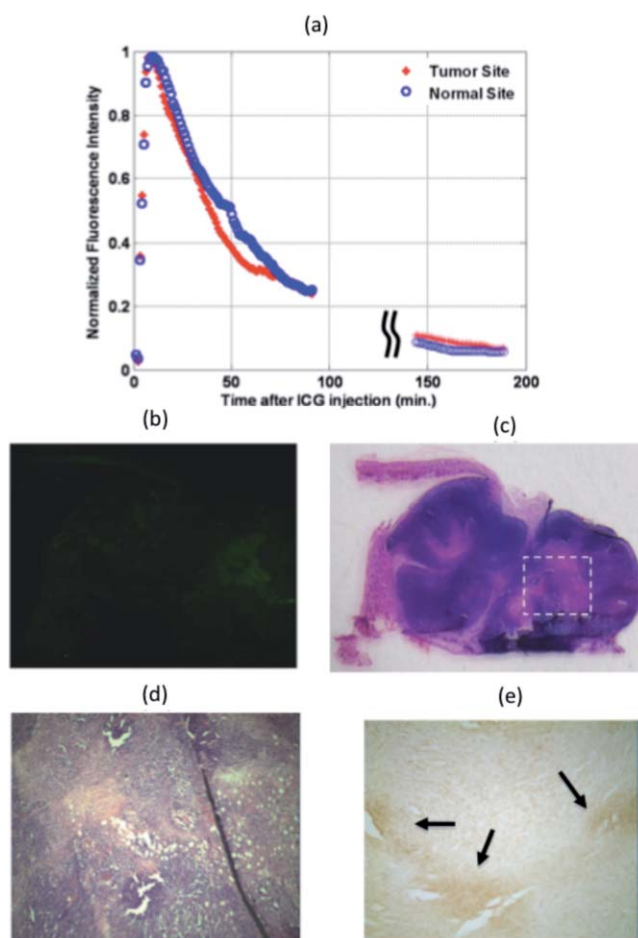


Fig. 2 Mouse injected with ICG and tumor size of 10 mm \times 5 mm. (a) Fluorescence signal measured from both the tumor and normal sites. (b) Fluorescence image acquired with Li-COR scanner. (c) Corresponding H&E stain. (d) 40 \times H&E of the marked region in (c). (e) Corresponding 40 \times immuno-histochemistry stain (brown) for tumor hypoxia.

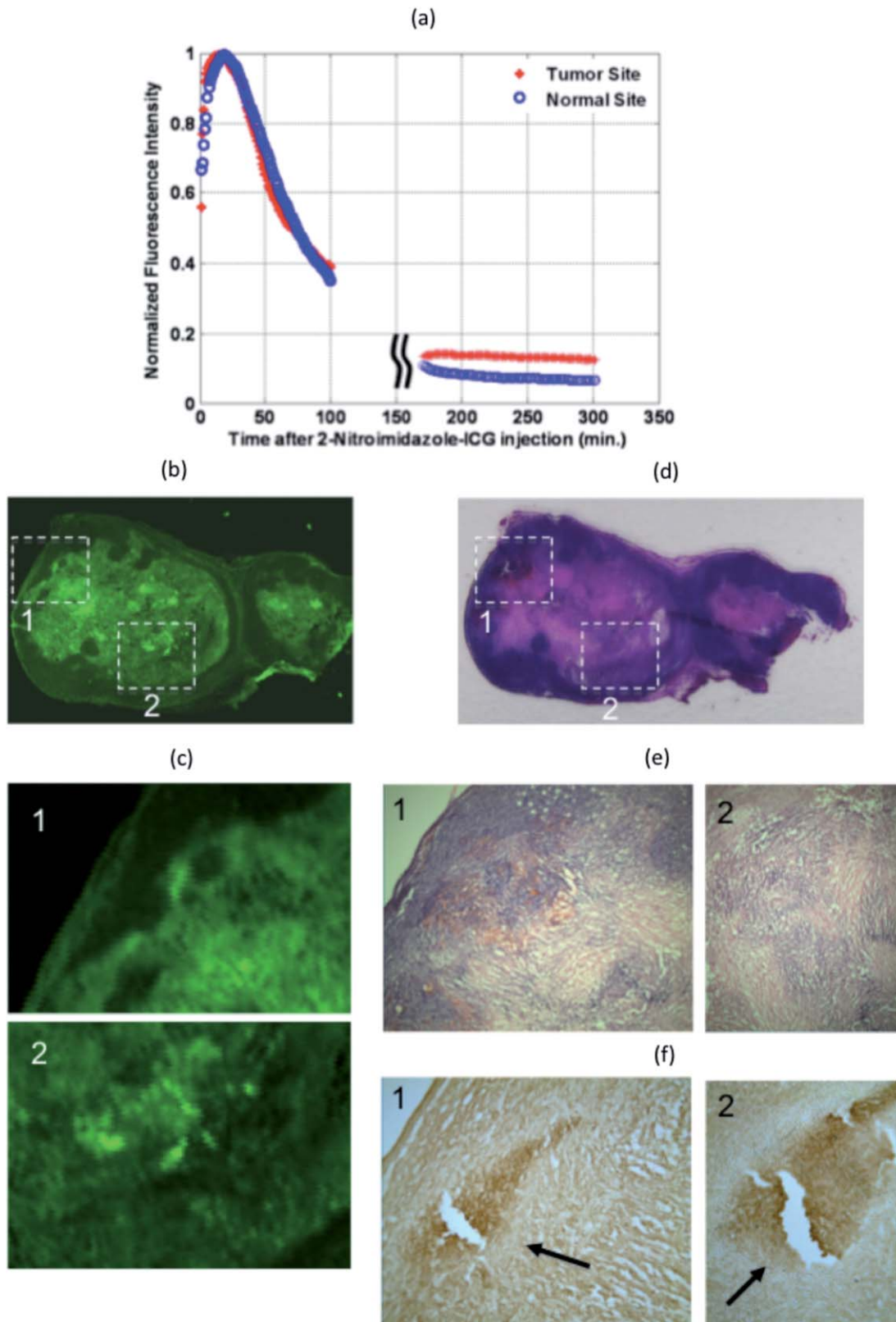


Fig. 3 Mouse injected with 2-nitroimidazole-ICG and tumor size of 10 mm×7 mm. (a) Fluorescence signal measured from both the tumor and normal sites. (b) Fluorescence image acquired with Li-COR scanner. (c) Magnified Li-COR scanner images of marked regions 1 and 2 in (b). (d) Corresponding H&E stain. (e) 40×H&E stain of the marked regions in (d). (f) Corresponding immuno-histochemistry stain (brown) for tumor hypoxia (1) 40×and (2) 100×magnification.

compound is about 2.5 times higher than normoxia, thus maintaining selectivity for hypoxia. However, the fluorescence intensity for ICG is about the same under hypoxia and normoxia conditions. Note that the difference between fluorescence intensity under hypoxia and normoxia conditions for 2-nitroimidazole-ICG at 500 nM concentration is reduced to less than 1.5 where it cannot be differentiated from ICG treated cells. The measurements for 2-nitroimidazole-ICG in hypoxic conditions were repeated on three different days to check the consistency of our findings, the results are labeled as “day 1,” “day 2,” and “day 3” for 2-Nitroimidazole ICG (Hypoxia) in Figs. 1(b) and 1(c).

In the first set of tumor uptake and dye wash out time experiments, ICG was injected into two mice with tumor sizes 9 mm×6 mm and 10 mm×8 mm, and 2-nitroimidazole-ICG was injected into two mice with tumor sizes 12 mm×6 mm and 10 mm×8 mm. The fluorescence emission was recorded simultaneously at both the tumor and contra-lateral normal sites. Two pairs of source-detector assemblies were placed on top of the tumor and the normal sites to measure the responses from the tumor and normal tissues, respectively. Source-detector separation was 10 mm for both pairs. The excitation wavelength was 690 nm and the power level was 18 mW. The fluorescence signal was collected by placing a band pass filter (HQ800/60 M, Chroma Technologies, Vermont) on the emission path.¹⁶ Equal volumes (100 μ l in PBS) of 10 μ M ICG were injected into two mice and 10 μ M 2-nitroimidazole-ICG were injected into the other two mice via supra orbital sinus under anesthesia. Background fluorescence and/or leak through the filter were recorded 3 min prior to injection. Immediately after injection, the fluorescence signals at both the tumor and normal sites increased rapidly. For ICG post-injection, the fluorescence signal reached peak in 7 to 10 min at both the tumor and normal sites. Using the 2-nitroimidazole-ICG conjugate, the fluorescence signal reached peak in 11 to 13 min and 8 to 17 min from the tumor and normal sites, respectively. The fluorescence signal was monitored for up to 100 min post-injection and again up to 300 min post-injection with intervening anesthesia breaks. The normalized fluorescence signals (after background subtraction) versus time of ICG injection for a mouse of tumor size 9 mm×6 mm are shown in Fig. 2(a). The normalized fluorescence signals versus time of 2-nitroimidazole-ICG injection for a mouse with tumor size of 10 mm×8 mm are shown in Fig. 3(a). For each mouse, the dye wash out curves up to 100 min at tumor and normal sites were the same. However, the fluorescence signal after approximately 150 min at the tumor site of the 2-nitroimidazole-ICG injected mouse was about 2.2 times higher on average than that at the normal site, while the fluorescence signal after approximately 150 min at both the tumor and normal sites of ICG injected mouse were about the same. Quantitatively, the ratios of 2.64 and 2.2 were found between fluorescence signals from tumor site and normal site for 2 mice injected with 2-nitroimidazole-ICG, and ratios of 1.1 and 1.3 were found for 2 mice injected with ICG. This suggests that the remaining higher fluorescence signals measured at tumor site of 2-nitroimidazole-ICG injected mice may be due to specific binding of the conjugate with tumor hypoxia areas. Figures 2(b) and 3(b) show the corresponding fluorescence images acquired with the Li-COR scanner of ICG and 2-nitroimidazole-ICG injected mice tumor samples, respectively. The tumor samples were harvested 6 h

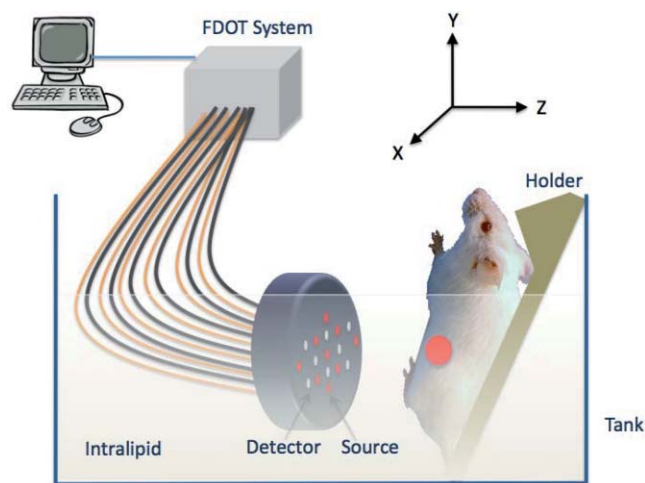


Fig. 4 *In vivo* fluorescence tomography imaging setup. The live mouse was submerged in 0.6% intralipid scattering medium.

after injection. Much higher fluorescence intensity was observed in the 2-nitroimidazole-ICG injected tumor sample than that of the ICG injected one. Figures 2(c) and 3(d) show the corresponding H&E stains of the ICG and 2-nitroimidazole-ICG injected mice tumor samples, respectively. Figures 2(d) and 3(e), which are 40× magnification of H&E stains from marked areas in Figs. 2(c) and 3(d), show that both tumors are similar with a significant amount of viable tumors and some necrosis areas. Figures 2(e) and 3(f) show immuno-histochemistry stains (brown) for hypoxia of corresponding areas revealing the presence of many scattered hypoxia areas as indicated by the arrows.

In the second set of fluorescence tomography imaging experiments, 9 source fibers and 8 detector fibers were distributed on a hand-held probe.¹⁶ During the experiments, mice were placed on a thin glass plate with the mammary fat-pad facing the imaging probe, as shown in Fig. 4. The center of the probe was aligned approximately to the center of the tumor and the head-to-tail of the mouse was along the Y-axis of the probe. The mouse was positioned at a fixed distance of 10 mm from the optical probe. For this set of imaging experiments, the probe-tumor contact was not a problem and the tumors studied were smaller than that of the first group. A dose of 100 μ l of 100 μ M ICG was injected to one mouse of tumor size 3 mm×4 mm and a dose of 100 μ l of 100 μ M 2-nitroimidazole-ICG was injected to two mice of tumor sizes 8 mm×4 mm and 6 mm×5 mm. The mice were imaged pre-injection, during, and post-injection at certain time intervals with intervening anesthesia breaks. Fluorescence tomography images of ICG and 2-nitroimidazole-ICG of mice of tumor sizes 3 mm×4 mm and 6 mm×5 mm are shown in Figs. 5(a) and 5(b), respectively, where the color bar represents the dye concentration in micromolars. ICG was completely washed out from the tumor site between 10 min and 3 h, but 2-nitroimidazole-ICG remained for more than 7 h in the tumor site. In Figs. 5(a) and 5(b), the second strong fluorescence target was the bladder, which was cleaned between 3 and 5 h for an ICG injected mouse and 5 to 7 h for a 2-nitroimidazole-ICG injected mouse. The data in Table 1 provides the reconstructed fluorophore concentrations for both cases and one additional mouse injected with 2-nitroimidazole-ICG. This example highlights the potential application of our novel 2-nitroimidazole-ICG for imaging tumor hypoxia after a

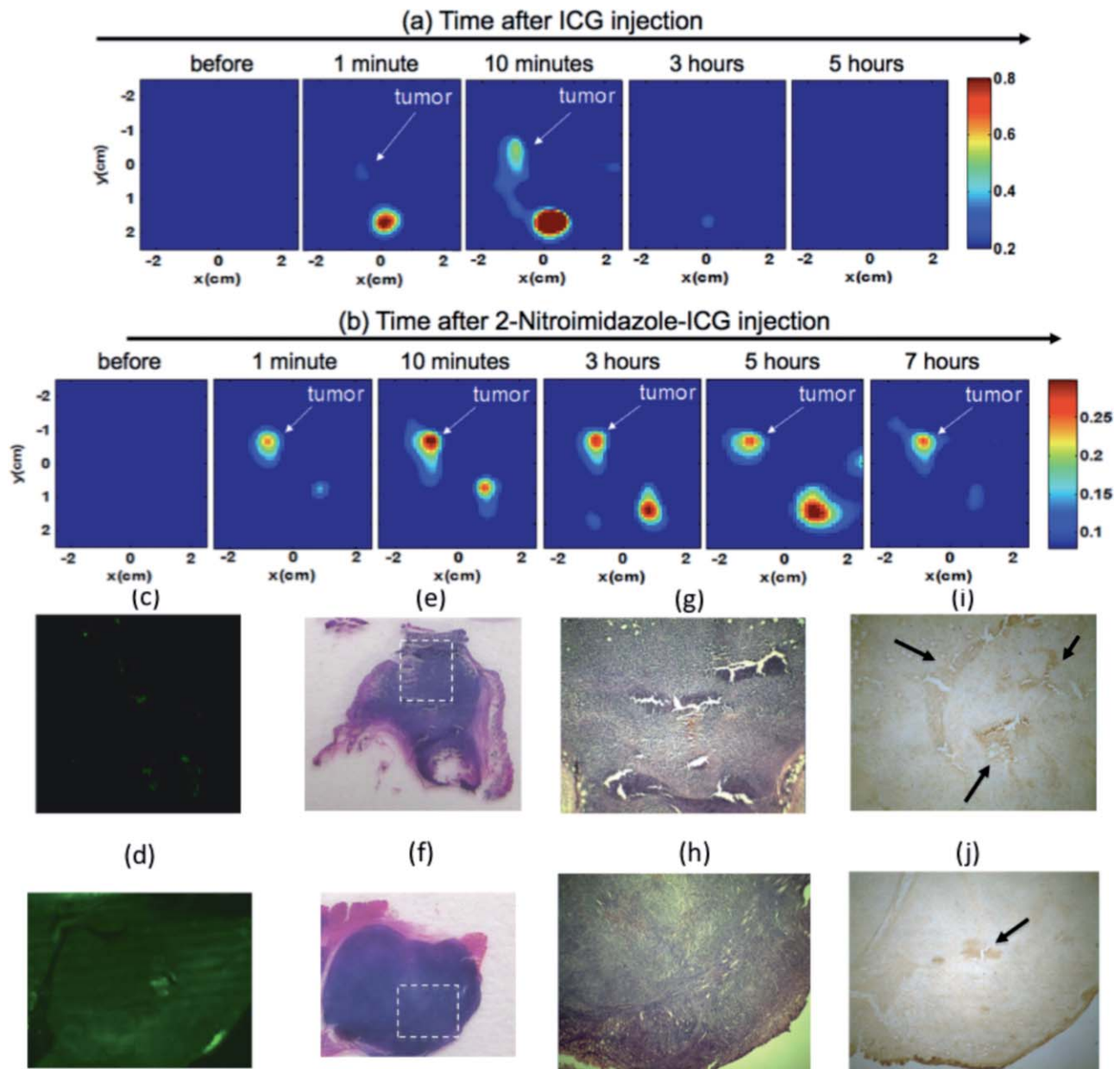


Fig. 5 Fluorescence tomography images obtained from (a) ICG injected mouse of tumor size 3 mm×4 mm and (b) 2-nitroimidazole-ICG injected mouse of tumor size 6 mm×5 mm. The color bars are the fluorophore concentration in micromolar. (a) For ICG; before, during and post-injection images. (b) For 2-nitroimidazole-ICG; before, during and post-injection images. (c) and (d) Fluorescence images acquired from Li-COR scanner of the ICG injected mouse and 2-nitroimidazole-ICG injected mouse. (e) and (f) Corresponding H&E stains. (g) and (h) 40×H&E of the marked region in (e) and (f), respectively. (i) and (j) Corresponding immuno-histochemistry stains (brown) for tumor hypoxia.

few hours of post-injection when the nontargeted dye has completely washed out. Figures 5(c) and 5(d) show the corresponding fluorescence images acquired with the Li-COR scanner of the ICG and 2-nitroimidazole-ICG injected mice tumor samples, respectively. A much higher fluorescence intensity was observed in the 2-nitroimidazole-ICG injected tumor sample than that in the ICG injected one. Figures 5(e) and 5(f) show the corresponding H&E stains of the ICG and 2-nitroimidazole-ICG injected mice tumor samples. Again, the 40×magnification images of the H&E stains [Figs. 5(g) and 5(h)], shows that the two tumors present a similar condition with a significant amount of viable tumors and no necrotic tissue. Figures 5(i) and 5(j) show

immunohistochemistry stains (brown) for hypoxia revealing the presence of hypoxia areas as indicated by the arrows.

Of the remaining one mouse injected with the 2-nitroimidazole-ICG with a tumor size 8 mm×4 mm, the fluorescence signal remained for more than 5 h post-injection in the tumor, and the bladder showed clearance between 3 to 5 h. The results are included in Table 1. We expect that this consistent selectivity is due to the specific accumulation of 2-nitroimidazoles in hypoxic tumors.

2-Nitroimidazole compounds are reduced in hypoxic cells and irreversibly bind to macromolecules (protein, nucleotides, etc.). The bound compounds would remain until cell metabolism

Table 1 Reconstructed dye concentrations of pre-injection and post-injection at certain time intervals. Unit is in micromolars.

Dye injected	Sites	Reconstructed dye concentration (μM) at different time					
		Pre-injection	Post-injection 1 min	10 min	3 h	5 h	7 h
ICG	Tumor	None	0.33	0.55	None	None	
	Bladder	None	0.83	1.2	0.3	None	
2-nitroimidazole-	Tumor	None	0.24	0.41	0.28	0.26	0.25
ICG	Bladder	None	0.18	0.27	0.37	0.44	0.12
2-nitroimidazole-	Tumor	None	None	0.32	0.41	0.30	
ICG	Bladder	None	1.04	0.54	0.38	0.19	

removed the macromolecules. It is well documented that the stability and half-life of the compound in the cells are dependent on cell type.²³ Different researchers have observed the turnover rates of hypoxic tumor cells with half-lives ranging from 17 to 49 h in various solid tumors. In a separate study, we have observed that the 2-nitroimidazole-ICG remained in a tumor, injected with 4T1 cell line, for 21 h and disappeared at 42 h post-injection. Future studies will investigate the optimal imaging window for the reported 2-nitroimidazole-ICG hypoxia probe.

4 Summary

In summary, we report the first *in vivo* animal experiments of a novel 2-nitroimidazole-ICG conjugate for noninvasive tumor hypoxia mapping using a near-infrared fluorescence imaging technique. We show that the fluorescence signals measured at the tumor site injected with 2-nitroimidazole-ICG was two-fold higher than that at the normal site after 150 min post-injection, while the fluorescence signals measured at the tumor site injected with ICG only was about the same as that measured at the normal site at the similar post-injection time. Fluorescence images acquired using a Li-COR commercial scanner on thin tumor samples confirmed a significantly higher dye accumulation for tumor samples injected with 2-nitroimidazole-ICG when compared to that of the ICG injected tumor. Immuno-histochemistry stains for tumor hypoxia using HypoxyprobeTM-1 showed the presence of tumor hypoxia areas. Post-injection fluorescence tomography images confirmed that the targeted 2-nitroimidazole-ICG remained for more than 5 to 7 h in tumors, however, the nontargeted ICG washed out from tumors in merely less than 3 h. Further investigations with a larger number of animals are warranted to validate the initial findings reported in this study. Additionally, the detection sensitivity and the imaging depth of our novel 2-nitroimidazole-ICG conjugate will be evaluated. The ultimate goal is to develop an *in vivo* hypoxia probe for mapping tumor oxygen conditions of advanced tumors and assessing treatment responses.

Acknowledgments

The authors thank the funding support of this work from the Connecticut Breast Health Initiative Inc., and Connecticut Public Health under Contract 2011-0141. The authors thank Professor Akiko Nishiyama and David Serwanski, Department of

Physiology and Neurobiology of the University of Connecticut, for their help on hypoxia staining using immunohistochemistry technique.

References

1. M. Hockel and P. Vaupel, "Tumor hypoxia: definitions and current clinical, biologic, and molecular aspects," *J. Natl. Cancer Inst.* **93**, 266–276 (2001).
2. A. L. Harris, "Hypoxia – a key regulatory factor in tumor growth," *Nat. Rev. Cancer* **2**, 38–47 (2002).
3. S. Kizaka-Kondoh, M. Inoue, H. Harada, and M. Hiraoka, "Tumor hypoxia: a target for selective cancer therapy," *Cancer Sci.* **94**, 1021–1028 (2003).
4. P. Vaupel, "Tumor microenvironmental physiology and its implications for radiation oncology," *Sem. Radiat. Oncol.* **14**, 198–206 (2004).
5. J. M. Brown and W. R. Wilson, "Exploiting tumor hypoxia in cancer treatment," *Nat. Rev. Cancer* **4**, 437–447 (2004).
6. M. Hockel, K. Schlenger, C. Knoop, and P. Vaupel, "Oxygenation of carcinomas of the uterine cervix: evaluation by computerized O₂ tension measurements," *Cancer Res.* **51**, 6098–6102 (1991).
7. D. M. Brizel, G. S. Sibley, L. R. Prosnitz, R. L. Scher, and M. W. Dewhurst, "Tumor hypoxia adversely affects the prognosis of carcinoma of the head and neck," *Int. J. Radiat. Oncol. Biol. Phys.* **38**, 285–289 (1997).
8. S. Kizaka-Kondoh and H. Konse-Nagasawa, "Significance of nitroimidazole compounds and hypoxia-inducible factor-1 for imaging tumor hypoxia," *Cancer Sci.* **100**(8), 1366–1373 (2009).
9. J. S. Rasey, G. V. Martin, and K. A. Krohn, "Quantifying hypoxia with radiolabeled fluoromisonidazole: pre-clinical and clinical studies," in the *The Imaging of Hypoxia*. H. J. Machulla, Ed., Kluwer Academic Publishers, Dordrecht, The Netherlands, pp. 85–117 (1999).
10. P. Zanzonico, J. O'Donoghue, J. D. Chapman, R. Schneider, S. Cai, S. Larson, B. Wen, Y. Chen, R. Finn, S. Ruan, L. Gerweck, J. Humm, and C. Ling, "Iodine-124-labeled iodo-azomycin-galactoside imaging of tumor hypoxia in mice with serial microPET scanning," *Eur. J. Nucl. Med. Mol. Imag.* **31**, 117–128 (2004).
11. J. Raleigh, A. Franko, D. Kelly, L. Trimble, and P. Allen, "Development of an *in vivo* 19F MR method for measuring oxygen deficiency in tumors," *Magn. Reson. Med.* **22**, 451–466 (1991).
12. D. J. Hawrysz and E. M. Sevick-Muraca, "Developments toward diagnostic breast cancer imaging using near-infrared optical measurements and fluorescent contrast agents," *Neoplasia* **2**(5), 388–417 (2000).
13. V. Ntziachristos, A. G. Yodh, M. Schnall, and B. Chance, "Concurrent MRI and diffuse optical tomography of breast after indocyanine green enhancement," *Proc. Natl. Acad. Sci. U.S.A.* **97**, 2767–2772 (2000).

14. J. A. N. Fisher, E. F. Civillico, D. Contreras, and A. G. Yodh, "in vivo fluorescence microscopy of neuronal activity in three dimensions by use of voltage-sensitive dyes," *Opt. Lett.* **29**, 71–73 (2004).
15. A. Corlu, R. Choe, T. Durduran, M. A. Rosen, M. Shweiger, S. R. Arridge, M. D. Schnall, and A. J. Yodh, "Three-dimensional in vivo fluorescence diffuse optical tomography of breast cancer in humans," *Opt. Exp.* **15**(11), 6696–6716 (2007).
16. N. C. Biswal, J. K. Gamelin, B. Yuan, M. V. Backer, J. M. Backer, and Q. Zhu, "Fluorescence imaging of vascular endothelial growth factor in tumors for mice embedded in a turbid medium," *J. Biomed Opt.* **15**(1), 016012 (2010).
17. N. C. Biswal, C. Pavlik, M. Smith, L. T. Kuhn, K. P. Claffey, and Q. Zhu, "Nitroimidazole-Indocyanine Green Conjugates for Breast Cancer Hypoxia Imaging," in *Biomedical Optics*, OSA Technical Digest (CD), paper JMA92, Optical Society of America (2010).
18. C. Pavlik, N. C. Biswal, F. C. Gaenzler, M. D. Morton, L. T. Kuhn, K. P. Claffey, Q. Zhu, and M. B. Smith, "Synthesis and fluorescent characteristics of imidazole-indocyanine green conjugates," *Dyes and Pigments* **89**, 9–15 (2011).
19. C. B. Allen, B. K. Schneider, and C. W. White, "Limitations to oxygen diffusion and equilibration in in-vitro cell exposure systems in hyperoxia and hypoxia," *Am. J. Physiol. Lung Cell Mo. Physiol.* **281**, L1021–L1027 (2001).
20. www.licor.com/bio/products/imaging_systems/odyssey/odyssey_imager.jsp
21. X. Li, D. R. Serwanski, C. P. Miralles, K. Nagata, and A. L. De Blas, "Septin 11 is present in GABAergic synapses and plays a functional role in the cytoarchitecture of neurons and GABAergic synaptic connectivity," *J. Biol. Chem.* **284**(25), 17253–17265 (2009).
22. M. Komitova, X. Zhu, D. R. Serwanski, and A. Nishiyama, "NG2 cells are distinct from neurogenic cells in the postnatal mouse subventricular zone," *Comp. Neurol.* **512**(5), 702–16 (2009).
23. A. S. Ljungkvist, J. Bussink, J. H. Kaanders, P. F. Rijken, A. C. Begg, J. A. Raleigh, and A. J. Van der Kogel, "Hypoxic cell turnover in different solid tumor lines," *Int. J. Radiat. Oncol. Biol. Phys.* **62**, 1157–1168 (2005).